Zn^{2+} Binding Properties of Single-Point Mutants of the C-Terminal Zinc Finger of the HIV-1 Nucleocapsid Protein: Evidence of a Critical Role of Cysteine 49 in Zn^{2+} Dissociation†

E. Bombarda,‡ H. Cherradi,‡ N. Morellet,§ B. P. Roques,§ and Y. Mély*,‡

Laboratoire de Pharmacologie et Physico-Chimie des Interactions Cellulaires et Moléculaires, UMR 7034 CNRS, Faculté de Pharmacie, Université Louis Pasteur, Strasbourg 1, 74, Route du Rhin, 67401 Illkirch Cedex, France, and Département de Pharmacochimie Moléculaire et Structurale, INSERM U266, CNRS UMR 8600, Faculté de Pharmacie, 4, Avenue de l'Observatoire, 75270 Paris Cedex 06, France

Received November 16, 2001; Revised Manuscript Received February 1, 2002

ABSTRACT: The two highly conserved Zn^{2+} finger motifs of the HIV-1 nucleocapsid protein, NCp7, strongly bind Zn^{2+} through coordination of one His and three Cys residues. To further analyze the role of these residues, we investigated the Zn^{2+} binding and acid−base properties of four single-point mutants of a short peptide corresponding to the distal finger motif of NCp7. In each mutant, one Zn^{2+}-coordinating residue is substituted with a noncoordinating one. Using the spectroscopic properties of Co^{2+}, we first establish that the four mutants retain their ability to bind a metal cation through a four- or five-coordinate geometry with the vacant ligand position(s) presumably occupied by water molecule(s). Moreover, the pK_a values of the three Cys residues of the mutant apopeptide where His44 is substituted with Ala are found by ^{1}H NMR to be similar to those of the native peptide, suggesting that the mutations do not affect the acid−base properties of the Zn^{2+}-coordinating residues. The binding of Zn^{2+} was monitored by using the fluorescence of Trp37 as an intrinsic probe. At pH 7.5, the apparent Zn^{2+} binding constants (between 1.6×10^8 and 1.3×10^{10} M^{-1}) of the four mutants are strongly reduced compared to those of the native peptide but are similar to those of various host Zn^{2+} binding proteins. As a consequence, the loss of viral infectivity following the mutation of one Zn^{2+}-coordinating residue in vivo may not be related to the total loss of Zn^{2+} binding. The pH dependence of Zn^{2+} binding indicates that the coordinating residues bind Zn^{2+} stepwise and that the free energy provided by the binding of a given residue may be modulated by the entropic contribution of the residues already bound to Zn^{2+}. Finally, the pK_a of Cys49 in the holopeptide is found to be 5.0, a value that is at least 0.7 unit higher than those for the other Zn^{2+}-coordinating residues. This implies that Cys49 may act as a switch for Zn^{2+} dissociation in the distal finger motif of NCp7, a feature that may contribute to the high susceptibility of Cys49 to electrophilic attack.

Processing products of the retroviral Gag polyprotein invariably include nucleocapsid proteins (NC) that, with the exception of spumaretrovirus (*1*), contain one or two copies of a zinc finger motif characterized by the sequence C-X_2-C-X_4-H-X_4-C (X being a variable amino acid residue) and thus also called the CCHC motif (*2*). In human immunodeficiency virus type 1 (HIV-1), the nucleocapsid protein NCp7 is characterized by two CCHC motifs that strongly coordinate Zn^{2+} in mature viruses (*3*, *4*). When Zn^{2+} binds, the protein changes from an unfolded to a stable and highly constrained structure (*3*, *5*, *6*).

Moreover, Zn^{2+} coordination seems to be necessary for most protein functions. For instance, numerous mutational studies have shown that the NC zinc finger domain, as a part of Gag precursor protein, is required for the selective recognition and packaging of genomic RNA into new virus particles (*6*−*15*). Moreover, since several mutations of the Zn^{2+}-coordinating residues lead to a much greater defect in infectivity than in genomic packaging (*7*, *11*−*14*, *16*, *17*) and since the antiviral activity of mimics of the Zn^{2+} finger motifs is thought to be linked to the impairment of reverse transcription (*18*), it is likely that the function of the CCHC motifs is not limited to the encapsidation step. In this respect, an increasing amount of evidence shows that the finger motifs are also involved in the nucleic acid chaperone activity of NCp7, especially during the reverse transcription step (*19*−*24*). This may explain the greatly reduced level of viral DNA synthesized by HIV-1 mutants with altered CCHC motifs (*14*, *17*).

The critical involvement of NCp7 zinc fingers in the HIV-1 replication cycle and their nonpermissive nature with respect to mutations have motivated the examination of the zinc fingers as targets for antiviral therapy. In this respect, various electrophilic compounds leading to HIV-1 inhibition by covalent modification of the nucleophilic zinc finger Cys

† This work was supported by grants from the Agence Nationale de Recherches sur le SIDA, SIDACTION, Centre National de la Recherche Scientifique, and Université Louis Pasteur.

* To whom correspondence should be addressed. Telephone: +33 (0)3 90 24 42 63. Fax: +33 (0)3 90 24 43 12. E-mail: mely@pharma.u-strasbg.fr.

‡ Université Louis Pasteur.

§ CNRS UMR 8600.

10.1021/bi015956g CCC: $22.00
Published on Web 03/07/2002

H-GCWKCGKEGHQMKDCT-OH	(35-50)NCp7
H-G**S**WKCGKEGHQMKDCT-OH	Ser36(35-50)NCp7
H-GCWK**S**GKEGHQMKDCT-OH	Ser39(35-50)NCp7
H-GCWKCGKEG**A**QMKDCT-OH	Ala44(35-50)NCp7
H-GCWKCGKEGHQMKD**S**T-OH	Ser49(35-50)NCp7

FIGURE 1: Amino acid sequence of (35−50)NCp7 derivatives.

thiolates have been identified (*25*−*29*). The two NCp7 zinc fingers, as well as each Cys residue, are not equally vulnerable to these agents. It has been established that reactions occur preferentially at the C-terminal zinc finger (*30*, *31*) and Cys49 is the most susceptible residue to electrophilic attack (*31*−*33*). Nevertheless, though some agents appear to react selectively with NCp7 zinc fingers (*34*), it remains unclear if NCp7 can be specifically targeted in vivo.

To design new strategies aimed at impairing Zn^{2+} binding, it is necessary to further understand the mechanism of Zn^{2+} coordination by NCp7. In this respect, we have recently characterized the Zn^{2+} binding properties of the C-terminal CCHC motif of NCp7 (*35*), taken as a relevant model of the retroviral CCHC motifs (*36*). The metal coordination has been shown to be extremely pH dependent due to a competition between protons and Zn^{2+} for the four coordinating residues. Moreover, the pK_a values of these residues in the apopeptide suggest an almost sequential deprotonation and thus a stepwise binding of Zn^{2+} to these residues. In addition, each protonation step of the coordination complex has been shown to decrease the Zn^{2+} binding constant by ∼4 orders of magnitude, a feature that may enable a significant dissociation of Zn^{2+} from the holopeptide in acidic cell compartments. To further understand the role of each coordinating residue in the binding of Zn^{2+} to the C-terminal CCHC motif of NCp7, we investigated herein the Zn^{2+} binding parameters of four single-point mutants of a short peptide, (35−50)NCp7, corresponding to the distal finger motif of NCp7. In each mutant, one Zn^{2+}-coordinating residue is substituted with a noncoordinating one. Moreover, each peptide includes the naturally occurring Trp37 that allows monitoring of Zn^{2+} binding by fluorescence spectroscopy. Our results reveal that the mutants are able to bind Zn^{2+} with a rather high affinity. Moreover, Zn^{2+} dissociation is found to be initiated at the Cys49 site, a feature that may contribute to the high susceptibility of this residue to electrophilic agents.

MATERIALS AND METHODS

Materials. (35−50)NCp7 derivatives (Figure 1) were synthesized in their apo form by solid-phase chemistry (*37*). The purity of the peptides was assessed by mass spectrometry to be higher than 98%. To preserve the highly oxidizable Cys residues, the lyophilized peptides were dissolved in freshly degassed buffer and immediately poured into anaerobic quartz cells, which maintain an inert argon atmosphere. The buffers were chosen as a function of the required pH: *N*,*N*′-diethyl-*N*,*N*′-bis(sulfopropyl)ethylenediamine (DESPEN) for pH 4.5−5.6, 2-(*N*-morpholino)ethanesulfonic acid (MES) for pH 5.6−6.8, 4-(2-hydroxyethyl)piperazine-1-ethanesulfonic acid (HEPES) for pH 6.8−8.5, and 2-(cyclohexylamino)ethanesulfonic acid (CHES) for pH 8.5−10. The buffer concentration was 50 mM. The ionic strength of all solutions was kept constant at 0.1 M by addition of $NaClO_4$. The perchlorate anions were chosen to minimize interactions with free or bound metal cations. The absence of peptide oxidation was checked at the end of each experiment by titration of the −SH content with 5,5′-dithiobis(2-nitrobenzoic acid) (DTNB) (*38*). Peptide concentrations were determined using an extinction coefficient of 5700 M^{-1} cm^{-1} at 280 nm.

Spectroscopic Measurements. The Co^{2+} complexes were formed in anaerobic quartz cells with a peptide concentration of 60−100 μM. The absorption spectra were recorded on a Cary 400 spectrophotometer and corrected for the contribution of the absorbance of the peptide.

The apparent Zn^{2+} binding constants (K_{app}) were determined at 20 ± 0.5 °C from fluorimetric titrations in anaerobic quartz cells with a thermostated SLM48000 spectrofluorimeter. Increasing $ZnSO_4$ or $Zn(ClO_4)_2$ concentrations were added to 10 μM peptide in 50 mM buffer, at an ionic strength of 0.1 M and at the desired pH. Chelator (1 mM) was used to buffer small concentrations of free Zn^{2+} when high affinity was expected. Ethylene glycol *O*,*O*′-bis(2-aminoethyl)-*N*,*N*,*N*′,*N*′-tetraacetic acid (EGTA) was used as a chelator for Ser49(35−50)NCp7 and Ala44(35−50)NCp7. 1,6-Diaminohexane-*N*,*N*,*N*′,*N*′-tetraacetic acid was used for Ser36-(35−50)NCp7 and Ser39(35−50)NCp7. At pH <6, the K_{app} values were low enough to avoid the addition of chelator. For each addition of Zn^{2+}, the fluorescence intensity changes at the maximum emission wavelength (350 nm) were followed for 5−15 min, to ensure that equilibrium was attained. Excitation was set at 280 nm. Excitation and emission bandwidths were 2 and 8 nm, respectively. The apparent Zn^{2+} binding constants were calculated from the fluorimetric titrations according to the methods of refs *35* and *36*.

To investigate the pH dependence of the fluorescence of the Zn^{2+}-bound (35−50)NCp7 derivatives, each peptide was dissolved at 10 μM in a mixture of 30 mM DESPEN, 15 mM MES, 15 mM HEPES, and 15 mM CHES to cover the pH range of 4.4−9. The ionic strength was 0.1 M. The progressive acidification of the solution was achieved with aliquots of diluted HCl. At each pH, at least 95% of the peptide was kept in its holo form by adding suitable amounts of excess Zn^{2+}.

^{1}H NMR Measurements. The Ala44(35−50)NCp7 peptide was dissolved in the presence of 100 mM NaCl in H_2O and 10% D_2O to give a final concentration of ∼2 mM. Two-dimensional phase-sensitive ^{1}H Clean-TOCSY with a spin lock of 70 ms (*39*) and NOESY with a mixing time of 100 ms (*40*) using time-proportional phase incrementation (TPPI) (*41*) were carried out at 293 K on an Avance Bruker spectrometer operating at 400.13 MHz without sample spinning with 2K real points in t_2 with a spectral width of 6000 Hz and 512 t_1 increments. The NOESY spectrum was recorded at pH 3.3, and TOCSY spectra were recorded at pH 3.3−10.9. The transmitter frequency was set to the water signal, which was suppressed by irradiation during the relaxation delay of 1.6 s between FIDs. The data were processed using UXNMR software (Brüker). A π/6 phase-shifted sine bell window function was applied prior to Fourier transformation in both dimensions (t_1 and t_2). The pH was increased by addition of small amounts of 0.1 M NaOH.

Table 1: Apparent Equilibrium Constants, K_{app} (M^{-1}), for the Binding of Zn^{2+} to (35−50)NCp7 Derivatives at pH 7.5[a]

Ser36(35−50)NCp7	Ser39(35−50)NCp7	Ala44(35−50)NCp7	Ser49(35−50)NCp7	(35−50)NCp7[b]
$(1.6 \pm 0.4) \times 10^8$	$(1.6 \pm 0.3) \times 10^8$	$(1.3 \pm 0.1) \times 10^{10}$	$(5.0 \pm 0.3) \times 10^9$	$(3.2 \pm 0.2) \times 10^{12}$

[a] The experiments were performed as described in Materials and Methods. The K_{app} values are expressed as means ± standard deviations for at least three independent titrations. [b] From ref *35*.

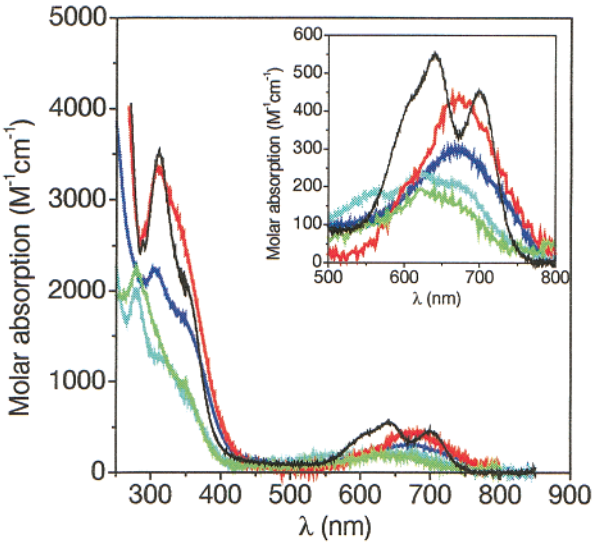

FIGURE 2: Corrected absorption spectra of the complexes of (35−50)NCp7 derivatives with Co^{2+}. The complexes were prepared with a 5-fold excess of Co^{2+}. The absorbance spectra were recorded with (35−50)NCp7 (black), Ser36(35−50)NCp7 (light blue), Ser39(35−50)NCp7 (green), Ala44(35−50)NCp7 (red) and Ser49(35−50)-NCp7 (blue). The inset shows an enlargement of the visible region.

RESULTS

To further understand the role of each coordinating residue in the binding of Zn^{2+} to the C-terminal zinc finger motif of NCp7, we synthesized four single-point mutants of the (35−50)NCp7 peptide where each Zn^{2+}-coordinating residue was individually substituted with a noncoordinating one (Figure 1). Serine was chosen as a replacement for cysteine since these two residues differ only by the substitution of an oxygen for a sulfur atom. To minimally perturb the protein conformation, histidine was changed to alanine, a residue that is found in buried as well as solvent-exposed positions of all secondary structures (*42*).

Determination of the Coordination Geometry in the Single-Point Mutants. The effect of each mutation on metal binding was first examined by taking advantage of the spectroscopic properties of Co^{2+}-substituted proteins. Since the ionic radius and the polarizability of the optically active Co^{2+} are similar to those of the spectroscopically silent Zn^{2+}, Co^{2+} is a convenient probe for providing information about the nature of the first coordination sphere of Zn^{2+} proteins (*43*, *44*). The corrected absorption spectra of the Co^{2+} complexes of (35−50)NCp7 and the four single-point mutants are given in Figure 2. The intense absorption in the near-UV region can be assigned to $S^- \rightarrow Co^{2+}$ ligand-to-metal charge transfer (LMCT) absorption. The intensity of this absorption in the Co^{2+} complex of (35−50)NCp7 and Ala44(35−50)NCp7 complexes is consistent with the presence of three Cys residues in the first shell of ligands (*45*). Moreover, the intensity of this absorption is decreased by approximately one-third in the three remaining complexes in keeping with the substitution of a single Cys residue.

The absorption in the visible region represents d−d electronic transition and provides information about the geometry and ligand composition of the first coordination shell. The maximal extinction coefficients of Ala44(35−50)-NCp7 and Ser49(35−50)NCp7 are greater than 300 M^{-1} cm^{-1} and, thus, indicative of tetrahedral coordination (*43*, *44*, *46*). This suggests that tetrahedral binding has been retained in these mutants with the vacant ligand position presumably occupied by a molecule of water. However, both the spectrum shape and the wavelength of the maximal extinction coefficient of these mutants are suggestive of a more or less distorted tetrahedral geometry (*47*). The maximal extinction coefficients of Ser36(35−50)NCp7 and Ser39(35−50)NCp7 are ∼200 M^{-1} cm^{-1} and are thus between the upper limit of 150 M^{-1} cm^{-1} for five-coordinate complexes and the lower limit of 300 M^{-1} cm^{-1} for four-coordinate complexes (*46*). This implies that the extinction coefficients of the complexes of these two mutants with Co^{2+} may arise from either four- or five-coordinate complexes, or an equilibrium between the two. Accordingly, either one or two molecules of water may participate in the first coordination shell in the complexes of these two mutants with Co^{2+}.

Zn^{2+} Binding Properties of the Single-Point Mutants at pH 7.5. The binding of Zn^{2+} to the four (35−50)NCp7 single-point mutants was monitored at pH 7.5 by using the fluorescence intensity of the naturally occurring Trp37 residue. In each peptide, the uptake of Zn^{2+} induces a fluorescence increase, although to a significantly lesser extent than in the wild-type (35−50)NCp7 peptide. Moreover, the magnitude of the fluorescence increase upon Zn^{2+} binding differs among the peptides. The largest increase (2.2-fold) is measured for Ala44(35−50)NCp7. In contrast, increases of only 2-, 1.6-, and 1.3-fold are observed for Ser49(35−50)NCp7, Ser39(35−50)NCp7, and Ser36(35−50)NCp7, respectively.

As expected, the deletion of each Zn^{2+}-coordinating residue significantly reduces the stability of the Zn^{2+} complex as compared to the native (35−50)NCp7 peptide (Table 1). The highest degree of destabilization is induced by the substitution of Cys36 or Cys39. These substitutions lead to a decrease of 4 orders of magnitude in the apparent binding constant (K_{app}). In contrast, the substitution of Cys49 induces a decrease of only 3 orders of magnitude in K_{app}. Finally, the substitution of His44 with Ala induces an only 2 order of magnitude decrease in K_{app}, suggesting that the coordination of His to Zn^{2+} provides a lower stabilization energy than coordination of Cys residues. This conclusion is in keeping with the lower energy of binding of Zn^{2+} to His as compared to Cys (*48*).

Determination by ^1H NMR of the pK_a of the Zn^{2+}-Coordinating Residues of the Ala44(35−50)NCp7 Apopeptide. Like the wild-type (35−50)NCp7 peptide (*35*), each mutated peptide displays a strong pH dependence of K_{app} in the pH range of 4.4−10. This behavior is not surprising since

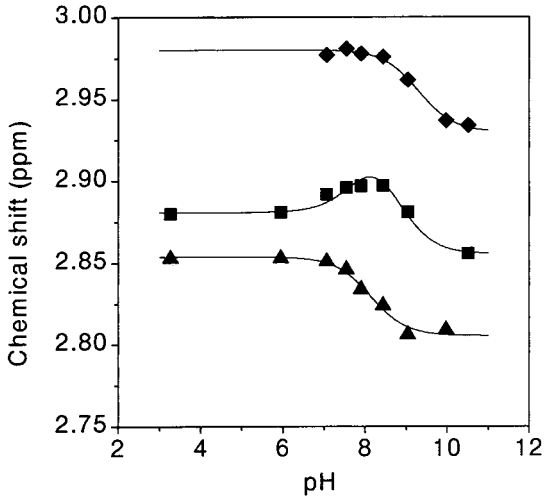

FIGURE 3: Variation of chemical shift with pH for cysteine Hβ protons of Ala44(35−50)NCp7. The data for Cys49 (◆) and Cys36 Hβ protons (▲) were fitted (solid line) with eq 1 and the parameters of Table 2. The data for the Cys39 Hβ proton (■) were fitted (solid line) with eq 2 and the parameters of Table 2.

each coordinating residue is thought to deprotonate before binding the metal cation. To check whether the pK_a values of the Zn^{2+}-coordinating residues of the mutated peptides are similar to those of the wild type, we determined by ^{1}H NMR spectroscopy the pK_a values of the Zn^{2+}-coordinating residues of the apopeptide form of Ala44(35−50)NCp7, taken as a representative mutant (Figure 3). In a first step, the proton resonances of the peptide were assigned at pH 3.3 using the procedures described by Wüthrich (*49*). In agreement with the observations for the (35−50)NCp7 apopeptide (*35*), the absence of medium- or long-range NOEs suggests that this mutated apopeptide is essentially random.

The pH titration of the thiol group of each cysteine was site-specifically investigated by monitoring the chemical shift of the resonances of the β protons used as a sensitive reporter of the deprotonation process (Figure 3). With the exception of Cys49, the distinction between the chemical shifts of the two Hβ protons of a given residue was not possible, in variance with the native (35−50)NCp7. This apparent difference is probably due to the use of a spectrometer operating at 400 MHz instead of 600 MHz. Nevertheless, the data show very strong similarities with the corresponding Cys residues of (35−50)NCp7 (*35*). In the case of Cys36 and Cys49, the pH dependence of the Hβ resonances is well fitted with a single pK_a, using the equation

$$\delta = \frac{\delta_{max} + \delta_{min} \times 10^{pH-pK_a}}{1 + 10^{pH-pK_a}} \quad (1)$$

where δ is the measured chemical shift at a given pH and δ_{max} and δ_{min} are the chemical shifts of the acidic and basic forms, respectively. The identity of the pK_a values with those of the corresponding Cys residues in the wild-type sequence (Table 2) strongly suggests that the substitution of His44 with Ala does not affect the protonation of the Cys residues, in line with the independence of the protonating groups (*35*). The similarities between Ala44(35−50)NCp7 and (35−50)-NCp7 are further underlined by the reproducibility of the anomalous pH dependence of the chemical shift of one Hβ proton of Cys39. Indeed, the profile of the titration curve of this proton indicates that at least two groups contribute to the variation of the chemical shift (Figure 3). An adequate fit of the experimental points is obtained with a model assuming a sequential titration of two noninteracting protonating groups:

$$\delta = \frac{\delta_0 + \delta_1 \times 10^{pH-pK_{a1}} + \delta_2 \times 10^{2pH-pK_{a1}-pK_{a2}}}{1 + 10^{pH-pK_{a1}} + 10^{2pH-pK_{a1}-pK_{a2}}} \quad (2)$$

where δ_0, δ_1, and δ_2 are the chemical shifts of the acidic, intermediate, and basic forms, respectively. The two pK_a values are 7.9 ± 0.3 and 8.7 ± 0.3. The more acidic pK_a is close to that of Cys36, while the most basic pK_a, by analogy to the wild type, can be attributed to the deprotonation of the thiol group of Cys39. This suggests that this Hβ proton in the Cys39 side chain acts as a reporter of the deprotonation of both the Cys36 and Cys39 thiol groups. In conclusion, our data strongly suggest that the protonation of a given Zn^{2+}-coordinating residue in a single-point mutant is similar to that of the corresponding residue in the native (35−50)-NCp7.

Table 2: pK_a Values of the Cysteine Residues of the Ala44(35−50)NCp7 Apopeptide, As Determined by ^{1}H NMR

residue		Ala44(35−50)NCp7[a]	(35−50)NCp7[b]
Cys36	Hβ1, Hβ2	8.1 ± 0.2	8.0 ± 0.2
Cys39	Hβ1	−	8.8 ± 0.2
	Hβ2	7.9 ± 0.3, 8.7 ± 0.3	8.2 ± 0.3, 8.7 ± 0.3
Cys49	Hβ1, Hβ2	9.3 ± 0.2	9.3 ± 0.2

[a] The pK_a values are expressed as the recovered value ± the error given by the fitting program based on the Levenberg−Marquardt algorithm. [b] Values from ref *35*.

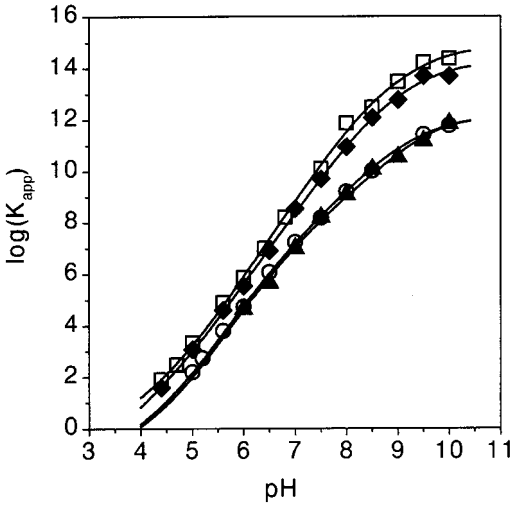

FIGURE 4: pH dependence of the apparent Zn^{2+} binding constant of the single-point mutants of (35−50)NCp7. The binding constants were measured at different pHs with a peptide concentration of 10 μM. Each experimental point of Ser36(35−50)NCp7 (○), Ser39-(35−50)NCp7 (▲), Ala44(35−50)NCp7 (□), and Ser49(35−50)-NCp7 (◆) corresponds to the mean of two or three individual titrations. Error bars are within the experimental points. The solid lines correspond to the fits with eq 3 and the data of Table 3.

pH Dependence of the Zn^{2+} Binding Properties of the Single-Point Mutants. In Figure 4, the apparent Zn^{2+} binding constant (K_{app}) of each single-point mutant is plotted as a function of pH. In line with the analysis of the binding of Zn^{2+} to the wild-type peptide, the equilibrium reaction

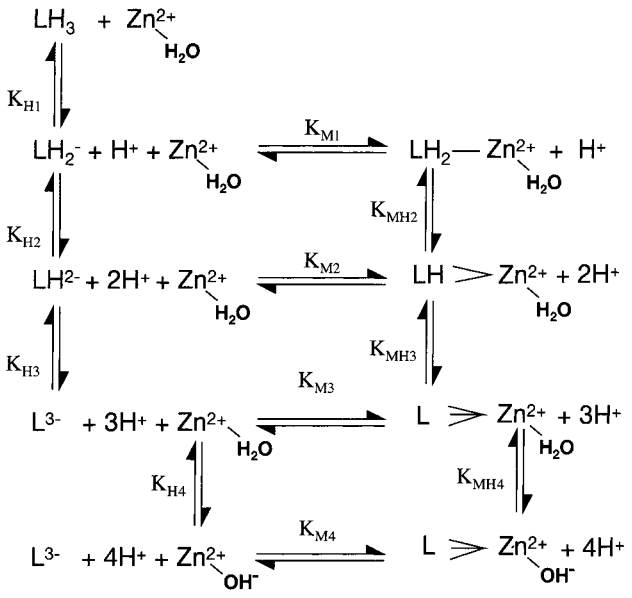

FIGURE 5: Scheme of Zn^{2+} binding to the single-point mutants of (35−50)NCp7. Only the Zn^{2+}-bound water molecule acting as a fourth coordinating residue in the holopeptide is indicated in the scheme.

scheme expected to describe metal binding to the single-point mutants from a macroscopic point of view is given in Figure 5. From this scheme, we can derive the following equation to account for the pH dependence of K_{app}:

$$K_{app} = \{K_{M4} + K_{M3}K_{H4}[H^+] + K_{M2}K_{H4}K_{H3}[H^+]^2 + K_{M1}K_{H4}K_{H3}K_{H2}[H^+]^3\}/\{1 + K_{H4}[H^+] + K_{H4}K_{H3}[H^+]^2 + K_{H4}K_{H3}K_{H2}[H^+]^3 + K_{H4}K_{H3}K_{H2}K_{H1}[H^+]^4\} \quad (3)$$

where the K_{Mi} constants represent the Zn^{2+} binding constants. The macroscopic protonation constants, K_{Hi}, of the various apopeptides (Table 3) are calculated from the pK_a values (Table 2) using a model accounting for noninteracting groups:

$$K_{H4} = k_{H1} + k_{H2} + k_{H3} + k_{H4} \quad (4)$$

$$K_{H3} = (k_{H1}k_{H2} + k_{H1}k_{H3} + k_{H1}k_{H4} + k_{H2}k_{H3} + k_{H2}k_{H4} + k_{H3}k_{H4})/K_{H4}$$

$$K_{H2} = (k_{H1}k_{H2}k_{H3} + k_{H1}k_{H2}k_{H4} + k_{H1}k_{H3}k_{H4} + k_{H2}k_{H3}k_{H4})/K_{H4}K_{H3}$$

$$K_{H1} = k_{H1}k_{H2}k_{H3}k_{H4}/K_{H4}K_{H3}K_{H2}$$

where $k_{Hi} = 10^{pK_a(X_i)}$, with X_i ($i = 1-3$) corresponding to the three intrinsic Zn^{2+}-coordinating residues of a given mutant. A pK_a of 6.4 was used for His44 when present (*35*). A pK_a of 10 was used for X_4 which corresponds to the zinc-bound water molecule, acting as the fourth coordinating residue (*50*).

The pH dependence of K_{app} for the various mutants was fitted with the logarithmic form of eq 3. Since it is expected that $K_{M4} > K_{M3} > K_{M2} > K_{M1}$, the numerator was progressively reduced to check if a good fit was still obtained. It results from this study that the parameters $K_{M2}-K_{M4}$ are necessary for a good fit over the investigated pH range. This suggests that in addition to the fully deprotonated L(OH^-)Zn species, both L(H_2O)Zn and LH(H_2O)Zn species may also be populated, at least in the most acidic part of the investigated pH range. In contrast, no significant amount of LH_2(H_2O)Zn seems to be present in the same pH range. The $K_{M2}-K_{M4}$ values are reported in Table 3. In keeping with the data at pH 7.5, the stability constant, K_{M4}, of the fully deprotonated peptide gives the following sequence: Ala44-(35−50)NCp7 > Ser49(35−50)NCp7 > Ser39(35−50)NCp7 ≡ Ser36(35−50)NCp7. In contrast, the comparison of the values of either K_{M2} or K_{M3} provides a slightly different order: Ala44(35−50)NCp7 > Ser49(35−50)NCp7 ≥ Ser36-(35−50)NCp7 > Ser39(35−50)NCp7. Noticeably, while the K_{M4}/K_{M3} ratio strongly varies among the mutants, the K_{M3}/K_{M2} ratio varies only within a factor of 3 among the various mutants.

Since the coordination geometry is uncertain for Ser36-(35−50)NCp7 and Ser39(35−50)NCp7, additional attempts were made to fit the experimental data of these two mutants with a model including two molecules of water as the fourth and fifth coordinating residues. A pK_a of 10 was assumed for both molecules. The K_{Hi} values were recalculated, and eq 3 was extended to include the stability constant, K_{M5}, of the L(OH^-)$_2$Zn species. In both peptides, the K_{M5} value was lower than the K_{M4} value, while the $K_{M2}-K_{M4}$ values were very similar to those calculated on the basis of a four-coordinate complex. This suggests that the putative fifth coordinating residue would only marginally stabilize the complexes of both mutants with Co^{2+}.

Finally, the protonation constants, K_{MH4} and K_{MH3}, of the holopeptide forms could be deduced from the following equation:

$$K_{MHi} = \frac{K_{Hi}K_{M(i-1)}}{K_{Mi}} \quad (5)$$

The values are reported in Table 3. The K_{MH4} values of the various mutants are much higher than the K_{MH4} value of the native holopeptide (*35*) and are in the range of the protonation constants of the Zn^{2+}-bound OH^- groups in the holo forms of various enzymes and model compounds with a similar number of thiolate and His ligands (*51*, *52*). It may thus be reasonably concluded that in keeping with our scheme in Figure 5, the step governed by K_{MH4} in the mutants is dominated by the acid−base properties of the Zn^{2+}-bound water molecule. In contrast, the K_{MH3} value is $\sim 10^5$ M^{-1} in all the mutants with the exception of Ser49(35−50)NCp7 and is thus close to the K_{MH4} value of the native holopeptide. This suggests that the associated step may be dominated by the acid−base properties of a Zn^{2+}-coordinating residue belonging to the peptide. According to the small K_{MH3} value of Ser49(35−50)NCp7 compared to those of the other mutants, this Zn^{2+}-coordinating residue may tentatively be ascribed to Cys49. Moreover, it results from the K_{MH3} values of the various mutants that the LH(H_2O)Zn species may only be populated at pH <6. In addition, since no significant amount of LH_2(H_2O)Zn may be present at pH >4.4, an upper limit of 1×10^4 M^{-1} can be assumed for K_{MH2}.

pH Dependence of the Fluorescence of the Zn^{2+}-Bound Mutated Peptides. In a previous work, we have observed that the quantum yield of Trp37 strongly depends on the

Table 3: Equilibrium Binding Parameters for the Binding of Zn^{2+} to the Single-Point Mutants of (35−50)NCp7

	Ser36(35−50)NCp7	Ser39(35−50)NCp7	Ala44(35−50)NCp7	Ser49(35−50)NCp7
K_{H1} (M^{-1})[a]	$(2.7 \pm 0.6) \times 10^6$	$(2.7 \pm 0.6) \times 10^6$	$(9 \pm 2) \times 10^7$	$(2.7 \pm 0.6) \times 10^6$
K_{H2} (M^{-1})[a]	$(5 \pm 1) \times 10^8$	$(1.1 \pm 0.4) \times 10^8$	$(6 \pm 2) \times 10^8$	$(1.0 \pm 0.4) \times 10^8$
K_{H3} (M^{-1})[a]	$(2.3 \pm 0.6) \times 10^9$	$(1.8 \pm 0.6) \times 10^9$	$(2.4 \pm 0.6) \times 10^9$	$(8 \pm 3) \times 10^8$
K_{H4} (M^{-1})[a]	$(1.3 \pm 0.1) \times 10^{10}$	$(1.2 \pm 0.1) \times 10^{10}$	$(1.3 \pm 0.1) \times 10^{10}$	$(1.1 \pm 0.1) \times 10^{10}$
K_{M1} (M^{-1})[b]	$\leq 2 \times 10^2$	$\leq 2 \times 10^2$	$\leq 6.0 \times 10^4$	$\leq 2 \times 10^2$
K_{M2} (M^{-1})[c]	$(1.0 \pm 0.7) \times 10^7$	$(1.3 \pm 0.8) \times 10^6$	$(6 \pm 2) \times 10^9$	$(1.5 \pm 0.5) \times 10^7$
K_{M3} (M^{-1})[c]	$(2.4 \pm 0.1) \times 10^{11}$	$(2.7 \pm 0.5) \times 10^{10}$	$(1.5 \pm 0.5) \times 10^{14}$	$(9.8 \pm 0.4) \times 10^{11}$
K_{M4} (M^{-1})[c]	$(1.2 \pm 0.2) \times 10^{12}$	$(1.4 \pm 0.3) \times 10^{12}$	$(7 \pm 2) \times 10^{14}$	$(1.7 \pm 0.2) \times 10^{14}$
K_{MH2} (M^{-1})[d]	$\leq 1 \times 10^4$	$\leq 1 \times 10^4$	$\leq 1 \times 10^4$	$\leq 1 \times 10^4$
K_{MH3} (M^{-1})[e]	$(9.6 \pm 0.5) \times 10^4$	$(8.7 \pm 0.5) \times 10^4$	$(1.0 \pm 0.2) \times 10^5$	$(1.2 \pm 0.2) \times 10^4$
K_{MH4} (M^{-1})[e]	$(2.6 \pm 0.5) \times 10^9$	$(2.3 \pm 0.2) \times 10^8$	$(3.0 \pm 0.5) \times 10^9$	$(6.3 \pm 0.5) \times 10^7$

[a] Proton binding constants are calculated with eq 4 from the pK_a values of Table 2 and assuming a pK_a of 10 for the Zn^{2+}-bound water molecule. [b] Calculated from eq 5 assuming that $K_{MH2} \leq 10^4$ M^{-1}. [c] Calculated from the fits of the experimental data of Figure 4 with eq 3. [d] Upper limit deduced from Figure 4. [e] Calculated from eq 5.

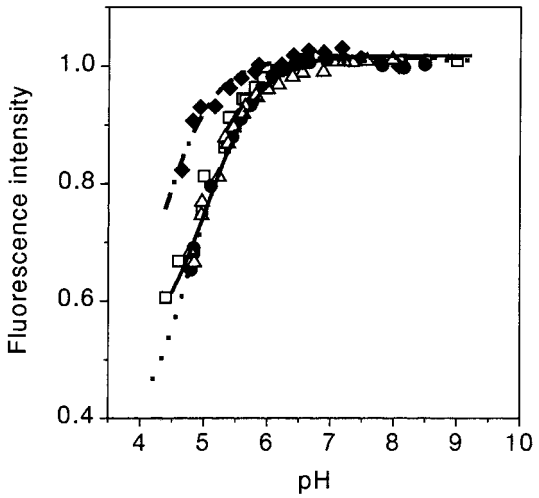

FIGURE 6: pH dependence of the fluorescence intensity of the Zn^{2+}-bound forms of the single-point mutants of (35−50)NCp7. The lines correspond to the fits of the experimental points of (35−50)NCp7 (□), Ser39(35−50)NCp7 (●), Ala44(35−50)NCp7 (△), and Ser49(35−50)NCp7 (◆) to eq 6.

folding of the holopeptide and decreases dramatically when the zinc-coordinating groups protonate (*35*). Moreover, it has been shown that the pH dependence of the fluorescence of the native (35−50)NCp7 holopeptide could be used to determine independently the K_{MH4} value. Herein, we apply the same approach to the holo forms of Ala44(35−50)NCp7, Ser39(35−50)NCp7, and Ser49(35−50)NCp7.

As for the native peptide, no fluorescence change is observed for the mutants in the pH range of 6−9 (Figure 6). Since the K_{MH4} values of the three peptides are between 6×10^7 and 3×10^9 M^{-1}, this indicates that no fluorescence change accompanies the protonation of the first Zn^{2+}-coordinating group in the holopeptide. This confirms that the first protonation step is dominated by the Zn^{2+}-bound OH^- group. Indeed, since this group does not belong to the peptide, its protonation is not expected to change the folding of the peptide around Zn^{2+} and hence Trp37 fluorescence.

At a more acidic pH, a dramatic fluorescence decrease of the three mutants is observed. However, while the pH dependence of the fluorescence intensities of both Ala44(35−50)NCp7 and Ser39(35−50)NCp7 holopeptides is strikingly similar to that of the native peptide, a clear shift toward a lower pH is observed for Ser49(35−50)NCp7. To fit the data of Figure 6, we use a reasoning similar to that in our previous paper (*35*). In short, since we are in the presence of saturating Zn^{2+} concentrations, the apopeptide concentration may be neglected. Moreover, since both $LH(H_2O)Zn$ and $LH_2(H_2O)Zn$ species are expected to be only partially structured, their fluorescence is assumed to be similar to that of the apopeptide. In contrast, since no fluorescence change could be observed in the pH range of 6−9, the fluorescences of the L(OH)Zn and $L(H_2O)Zn$ species are assumed to be identical. Finally, according to the binding data, the $LH_2(H_2O)Zn$ concentration is assumed to be negligible in the investigated pH range. It may thus be readily inferred that the ratio between the fluorescence, I, at a given pH and that at basic pH, $I_{L(OH)Zn}$, is given by

$$\frac{I}{I_{L(OH)Zn}} = \frac{1 + K_{MH4}[H^+] + \frac{I_L}{I_{L(OH)Zn}} K_{MH4}K_{MH3}[H^+]^2}{1 + K_{MH4}[H^+] + K_{MH4}K_{MH3}[H^+]^2} \quad (6)$$

Using the K_{MH4} value of Table 3, an excellent fit of the data of both Ser39(35−50)NCp7 and Ala44(35−50)NCp7 peptides is obtained with a K_{MH3} value of $(1.0 \pm 0.1) \times 10^5$ M^{-1}, in excellent agreement with the values recovered from the pH dependence of K_{app} (Table 3). Moreover, a K_{MH3} value of $(2 \pm 1) \times 10^4$ M^{-1} is obtained from the titration of Ser49(35−50)NCp7, again in excellent agreement with the data of Table 3.

DISCUSSION

Zinc finger motifs are classified as structural metal binding sites in which the Zn^{2+} coordination sphere is constituted exclusively by endogenous residues (*53*). In agreement with this classification, the high affinity of the distal finger motif of NCp7 for Zn^{2+} has been clearly related to the four Zn^{2+}-coordinating residues (*35*, *36*). To further analyze the role of each coordinating residue in the binding process, we report here the effects of independently mutating each of these residues to a noncoordinating residue. By using Co^{2+}, we have first established that both Ala44(35−50)NCp7 and Ser49(35−50)NCp7 mutants bind the metal cation through a distorted tetrahedral geometry with the vacant ligand position presumably occupied by a water molecule. A similar conclusion has been reached with a truncated C_2H zinc finger peptide (*54*) or a C_2H_2 peptide in which one His residue has been replaced with an alanine (*55*). In contrast, discrimination between four- and five-coordinate geometry could not be achieved for the complexes of Ser36(35−50)NCp7 and

Ser39(35−50)NCp7 with Co^{2+}. However, the Zn^{2+} binding data suggest that the molecule of water acting as a putative fifth coordinating residue would only marginally stabilize the complex and not affect our conclusions based on a model with four-coordinate geometry.

By ^1H NMR, we have additionally shown that the pK_a values of the three Cys residues of Ala44(35−50)NCp7 in its apo form are similar to those of the native (35−50)NCp7 apopeptide, suggesting that mutation of one coordinating residue does not affect the pK_a values of the remaining residues. This conclusion can be extended to the other mutants since an excellent fit of the pH dependence of K_{app} (Figure 4) is obtained in each case by using the pK_a values determined for the wild-type peptide. This last test is rather sensitive since simulations show that a shift of one pK_a by only 0.5 unit significantly decreases the quality of the fit (data not shown). By analogy to the native (35−50)NCp7 peptide (*35*), the anomalous behavior of one Hβ resonance of Cys39 in Ala44(35−50)NCp7 may be linked to the formation of a hydrogen bond network that weakly structures the Cys36−Cys39 segment. This structured segment may constitute an important feature for folding of the peptide by acting as a nucleation center.

The Zn^{2+} binding constants of the four single-point mutants at pH 7.5 are in the same range as those of the C_2H_2 motifs of eukaryotic transcription factors (*56*). They are also similar to the Zn^{2+} binding constants of various Zn^{2+}-containing enzymes (*57*). This feature was not unexpected since the catalytic sites of most Zn^{2+}-containing enzymes are also characterized by three protein ligands to zinc and an "open" fourth ligand position typically occupied by water or a hydroxide ion (*58*). As a consequence, the loss of viral infectivity that follows the substitution of one Zn^{2+}-coordinating residue with a noncoordinating one in vivo (*7*, *12*) may not be related to a total loss of Zn^{2+} binding. In contrast, preliminary ^1H NMR data (data not shown) and the differences in the fluorescence properties of Trp37 between the mutants and the native holopeptide suggest that the mutations induce large structural changes. This conclusion is in line with theoretical studies predicting that these mutations are expected to drastically degrade the native protein structure by disrupting the interior scaffold of NH−S bonds and coupled NH−O interactions (*59*). Large structural changes have also been evidenced when either His23 is replaced with Cys (*60*) or Cys28 is replaced with His (*61*) in the proximal finger motif. Both mutations have been shown to modify the folding around the metal atom and induce a loss of proximity between the two finger motifs and/or a change of the spatial orientation of the amino acid side chains critically involved in nucleic acid interaction. Moreover, the unusually high Zn^{2+} binding constants of the finger motifs of NCp7 have been recently linked to the need for NCp7 to outcompete the host proteins for the full zinc pool in the host cell (*62*). Since the affinity of the single-point mutants is at the same level as that of the host proteins, this may not be sufficient to allow their saturation by zinc and contribute to the loss of viral infectivity.

Additional information can be extracted from the pH dependence of K_{app}. Since the pK_a values of the Zn^{2+}-coordinating residues differ substantially from each other and are at least 0.7 unit lower than the pK_a value of the Zn^{2+}-bound water, it results that, as in the native peptide (*35*), the deprotonation of the Zn^{2+}-coordinating residues in the mutated apopeptides is almost sequential. This implies that K_{M3} describes the constant for binding of Zn^{2+} to the three intrinsic Zn^{2+}-coordinating residues in each mutant. Thus, the comparison of the K_{M3} value of a given mutant with the K_{M4} value of the native peptide provides a direct estimation of the free energy ($\Delta\Delta G^*$) associated with the binding of Zn^{2+} to the mutated coordinating residue (Table 4). The large free energy associated with the substitution of Cys39 is probably related to the small entropy gain resulting from this substitution. Indeed, the increase in the level of conformational freedom of the peptide segment in which Cys39 has been substituted is probably limited by the Cys36 and His44 residues which anchor this segment to Zn^{2+}. In contrast, a more dramatic increase in the flexibility is expected for the peptide segments in which either Cys36 or Cys49 has been substituted since in both the cases, the mutated segment is anchored to Zn^{2+} by only one coordinating residue.

Table 4: Free Energies (kJ/mol) Associated with the Various Steps of the Binding of Zn^{2+} to the Single-Point Mutants of (35−50)NCp7

	Ser36-(35−50)-NCp7	Ser39-(35−50)-NCp7	Ala44-(35−50)-NCp7	Ser49-(35−50)-NCp7
$\Delta\Delta G_1$[a]	−12.9	−11.2	−26.8	−12.9
$\Delta\Delta G_{1\rightarrow2}$[a]	−26.3	−23.1	−28.0	−27.3
$\Delta\Delta G_{2\rightarrow3}$[a]	−24.6	−24.2	−24.7	−27.0
$\Delta\Delta G_{3\rightarrow4}$[a]	−3.92	−9.61	−3.75	−12.6
$\Delta\Delta G^*$[b]	−28.3	−33.6	−12.6	−24.9

[a] $\Delta\Delta G_{i\rightarrow i+1}$ is the free binding energy associated with the binding of the *i*th coordinating residue to Zn^{2+} calculated with the equation $\Delta\Delta G_{i\rightarrow i+1} = -RT \ln(K_{Mi+1}/K_{Mi})$, where K_{Mi} and K_{Mi+1} are given in Table 3. [b] $\Delta\Delta G^*$ is the free energy associated with the substitution of a given Zn^{2+}-coordinating residue with a noncoordinating one and is calculated with the equation $\Delta\Delta G^* = -RT \ln(K_{M4}^{WT}/K_{M3})$, where K_{M4}^{WT} is the Zn^{2+} binding parameter for the fully deprotonated (35−50)NCp7 apopeptide (*35*) and K_{M3} is the Zn^{2+} binding parameter for a given single-point mutant.

From the comparison of K_{M3} with K_{M2} (Table 3), it appears that the stabilization (−24.2 to −27 kJ/mol) afforded by the binding of the third coordinating residue is in keeping with the free energy of Zn^{2+} binding to the thiolate group of free Cys (*48*). Furthermore, from the hypothesis that the K_{MH2} value is lower than 10^4 M^{-1}, we can also calculate an upper limit for K_{M1} (Table 3). This, in turn, enables us to calculate the stabilization energies associated with the binding of the first and second coordinating residues to Zn^{2+} (Table 4). In Ala44(35−50)NCp7, the energies (approximately −27 kJ/mol) associated with each step are consistent with the binding of Cys residues. A similar energy is associated with the binding of the second coordinating residue to Zn^{2+} in the remaining mutants, while a −11 to −13 kJ/mol energy is associated with the first one. This strongly suggests that in the latter mutants, the first step (governed by K_{M1}) of the scheme in Figure 5 is dominated by the binding of His44 to Zn^{2+}. Moreover, since the free energies inferred for the first Zn^{2+} binding step (Table 4) are in good agreement with the values expected from the sequential model, it is likely that K_{M1} is close to the upper limit reported in Table 3. Taken together, our data further substantiate the hypothesis that in agreement with the "zipper" model (*63*), the sequential deprotonation of the Zn^{2+}-coordinating residues may induce a stepwise binding to Zn^{2+} (*35*). Using this hypothesis, it

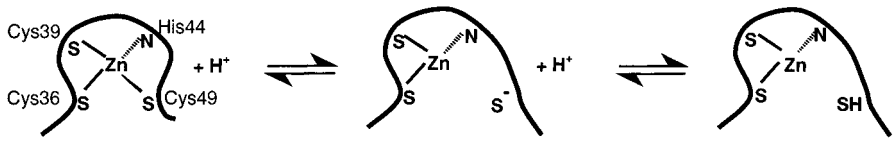

FIGURE 7: Schematic representation of the acid−base equilibrium of Cys49 in the (35−50)NCp7 holopeptide. The intermediate species with Cys49 in its thiolate form is thought to be highly susceptible to electrophilic agents. In addition, the protonation of Cys49 is thought to induce a conformational lability that may favor the access of the electrophilic agents.

could be further deduced from the comparison of the $\Delta\Delta G$ values in Table 4 that the stabilization afforded by a given residue may be modulated by the entropic contribution associated with the residues that are already bound to Zn^{2+}.

Both the high K_{MH4} value and the absence of fluorescence change associated with the first protonation step of the mutated holopeptides strongly suggest that this step mainly describes the protonation of the hydroxide ion bound to Zn^{2+}. Moreover, if we assume that the Zn^{2+}-coordinating groups protonate independently in the holopeptide, the K_{MHi} values may be expressed as

$$K_{MH4} = k_{MH1} + k_{MH2} + k_{MH3} + k_{MH4}$$

$$K_{MH3} = (k_{MH1}k_{MH2} + k_{MH1}k_{MH3} + k_{MH1}k_{MH4} + k_{MH2}k_{MH3} + k_{MH2}k_{MH4} + k_{MH3}k_{MH4})/K_{MH4} \quad (7)$$

$$K_{MH2} = (k_{MH1}k_{MH2}k_{MH3} + k_{MH1}k_{MH2}k_{MH4} + k_{MH1}k_{MH3}k_{MH4} + k_{MH2}k_{MH3}k_{MH4})/K_{MH4}K_{MH3}$$

where $k_{MHi} = 10^{pK_a(X_i)}$, with X_i ($i = 1-3$) corresponding to the intrinsic Zn^{2+}-coordinating residues and X_4 corresponding to the water molecule acting as the fourth coordinating residue. Since in all the mutants the K_{MH4} value is at least 1 order of magnitude higher than the K_{MH3} value (Table 3), it may be concluded from eq 7 that $K_{MH4} \approx k_{MH4}$ and, hence, K_{MH4} is directly connected to the pK_a of the Zn^{2+}-bound water molecule in the holopeptide. The K_{MH4} value of Ser36(35−50)NCp7 is fully consistent with the pK_a of bound water in enzymes or model compounds that also coordinate Zn^{2+} through two Cys residues and one His residue (*51*, *52*). In contrast, the significantly lower values measured with Ser39(35−50)NCp7 and Ser49(35−50)NCp7 may be related to the influence of a close positively charged Lys side chain that may increase the electrophilicity of the metal ion. The same explanation probably holds true for Ala44(35−50)NCp7 since its higher thiolate content was expected to lead to a much higher pK_a value for the Zn^{2+}-bound water molecule (*51*). Noticeably, since the K_{MH4} value of Ser49(35−50)NCp7 is 6×10^7 M^{-1} (corresponding to a pK_a of 7.8), a significant amount of Zn^{2+}-bound hydroxide is formed at physiological pH. This makes this peptide an attractive candidate as a catalytic tetrahedral Zn^{2+}-binding site that may be used in protein design to accelerate reactions involving hydroxide as a nucleophile.

Additionally, our data suggest that Cys49, when present, is the first intrinsic Zn^{2+}-coordinating residue that protonates in the holo form. Since the K_{MH3} values of the Cys49-containing mutants are analogous to the K_{MH4} value of the native peptide, the same conclusion may hold true for the native peptide. Furthermore, since the K_{MH3} value of Ser49-(35−50)NCp7 is at least 5 times lower than that of the other mutants (Table 3 and Figure 6), it may be approximated from eq 7 that $K_{MH3} \approx 10^{pK_a(Cys49)}$ in the Cys49-containing derivatives. It results that the pK_a of Cys49 is ∼5.0 in the holo form and is thus 4.3 units lower than in the apo form. This may be mainly attributed to the repulsive electrostatic interactions exerted by the positively charged cation toward protons (*64*) as well as to NH−S interactions that are thought to decrease the pK_a of Cys residues (*59*). In addition, from the K_{MH3} value of Ser49(35−50)NCp7, we further conclude that the pK_a values of Cys36, Cys39, and His44 could not exceed 4.3 in the holo form of the various (35−50)NCp7 derivatives.

One important consequence of our data is that Cys49 may act as a switch for Zn^{2+} dissociation in the distal finger motif of NCp7, especially if dissociation is induced by a pH decrease. Moreover, this critical function of Cys49 may additionally contribute to the high susceptibility of this residue to electrophilic attack. At pH 7.5, the percentage of protonated Cys49 is very low, being only ∼0.3% of the holopeptide population. However, for a given molecule, the holopeptide species with a protonated Cys49 residue are probably transient and cycle rapidly back to the fully deprotonated holopeptide form. As a consequence, every molecule is expected to go through this cycle with time. During this cycle, Cys49 may transiently appear in its free thiolate form (Figure 7) which is highly sensitive to electrophile agents and, thus, contributes to the high susceptibility of Cys49 to these agents (*31*−*33*). In addition, the protonation of Cys49 may also induce an increased conformational flexibility of the C-terminal end of the peptide. This hypothesis is consistent with the conformational flexibility of the distal finger motif observed by NMR (*65*). In addition to the large increase in the level of exposure of Cys49 which is related to the 60−75% lower electrostatic screening of this residue as compared to the other NCp7 thiolates (*59*), the increased flexibility of the C-terminal end of the peptide may further favor the steric access of Cys49 to electrophile agents.

ACKNOWLEDGMENT

We are indebted to Dr. Ernst Grell for fruitful discussion.

REFERENCES

1. Maurer, B., Bannert, H., Darai, G., and Flugel, R. M. (1988) *J. Virol. 62*, 1590−1597.
2. Berg, J. M. (1986) *Science 232*, 485−487.
3. Summers, M. F., Henderson, L. E., Chance, M. R., Bess, J. W., Jr., South, T. L., Blake, P. R., Sagi, I., Perez-Alvarado, G., Sowder, R. C. d., Hare, D. R., et al. (1992) *Protein Sci. 1*, 563−574.
4. Bess, J. W., Jr., Powell, P. J., Issaq, H. J., Schumack, L. J., Grimes, M. K., Henderson, L. E., and Arthur, L. O. (1992) *J. Virol. 66*, 840−847.
5. Morellet, N., Jullian, N., De Rocquigny, H., Maigret, B., Darlix, J. L., and Roques, B. P. (1992) *EMBO J. 11*, 3059−3065.

6. Morellet, N., de Rocquigny, H., Mely, Y., Jullian, N., Demene, H., Ottmann, M., Gerard, D., Darlix, J. L., Fournie-Zaluski, M. C., and Roques, B. P. (1994) *J. Mol. Biol. 235*, 287−301.
7. Aldovini, A., and Young, R. A. (1990) *J. Virol. 64*, 1920−1926.
8. Dupraz, P., Oertle, S., Meric, C., Damay, P., and Spahr, P. F. (1990) *J. Virol. 64*, 4978−4987.
9. Dupraz, P., and Spahr, P. F. (1993) *J. Virol. 67*, 3826−3834.
10. Schwartz, M. D., Fiore, D., and Panganiban, A. T. (1997) *J. Virol. 71*, 9295−9305.
11. Zhang, Y., and Barklis, E. (1995) *J. Virol. 69*, 5716−5722.
12. Dorfman, T., Luban, J., Goff, S. P., Haseltine, W. A., and Gottlinger, H. G. (1993) *J. Virol. 67*, 6159−6169.
13. Gorelick, R. J., Nigida, S. M., Jr., Bess, J. W., Jr., Arthur, L. O., Henderson, L. E., and Rein, A. (1990) *J. Virol. 64*, 3207−3211.
14. Gorelick, R. J., Gagliardi, T. D., Bosche, W. J., Wiltrout, T. A., Coren, L. V., Chabot, D. J., Lifson, J. D., Henderson, L. E., and Arthur, L. O. (1999) *Virology 256*, 92−104.
15. Berkowitz, R., Fisher, J., and Goff, S. P. (1996) *Curr. Top. Microbiol. Immunol. 214*, 177−218.
16. Gorelick, R. J., Chabot, D. J., Ott, D. E., Gagliardi, T. D., Rein, A., Henderson, L. E., and Arthur, L. O. (1996) *J. Virol. 70*, 2593−2597.
17. Tanchou, V., Decimo, D., Pechoux, C., Lener, D., Rogemond, V., Berthoux, L., Ottmann, M., and Darlix, J. L. (1998) *J. Virol. 72*, 4442−4447.
18. Druillennec, S., Dong, C. Z., Escaich, S., Gresh, N., Bousseau, A., Roques, B. P., and Fournie-Zaluski, M. C. (1999) *Proc. Natl. Acad. Sci. U.S.A. 96*, 4886−4891.
19. Remy, E., de Rocquigny, H., Petitjean, P., Muriaux, D., Theilleux, V., Paoletti, J., and Roques, B. P. (1998) *J. Biol. Chem. 273*, 4819−4822.
20. Rong, L., Liang, C., Hsu, M., Kleiman, L., Petitjean, P., de Rocquigny, H., Roques, B. P., and Wainberg, M. A. (1998) *J. Virol. 72*, 9353−9358.
21. Williams, M. C., Rouzina, I., Wenner, J. R., Gorelick, R. J., Musier-Forsyth, K., and Bloomfield, V. A. (2001) *Proc. Natl. Acad. Sci. U.S.A. 98*, 6121−6126.
22. Drummond, J. E., Mounts, P., Gorelick, R. J., Casas-Finet, J. R., Bosche, W. J., Henderson, L. E., Waters, D. J., and Arthur, L. O. (1997) *AIDS Res. Hum. Retroviruses 13*, 533−543.
23. Wu, W., Henderson, L. E., Copeland, T. D., Gorelick, R. J., Bosche, W. J., Rein, A., and Levin, J. G. (1996) *J. Virol. 70*, 7132−7142.
24. Guo, J., Wu, T., Anderson, J., Kane, B. F., Johnson, D. G., Gorelick, R. J., Henderson, L. E., and Levin, J. G. (2000) *J. Virol. 74*, 8980−8988.
25. Rice, W. G., Schaeffer, C. A., Harten, B., Villinger, F., South, T. L., Summers, M. F., Henderson, L. E., Bess, J. W., Jr., Arthur, L. O., McDougal, J. S., et al. (1993) *Nature 361*, 473−475.
26. Rice, W. G., Turpin, J. A., Schaeffer, C. A., Graham, L., Clanton, D., Buckheit, R. W., Jr., Zaharevitz, D., Summers, M. F., Wallqvist, A., and Covell, D. G. (1996) *J. Med. Chem. 39*, 3606−3616.
27. Rice, W. G., Baker, D. C., Schaeffer, C. A., Graham, L., Bu, M., Terpening, S., Clanton, D., Schultz, R., Bader, J. P., Buckheit, R. W., Jr., Field, L., Singh, P. K., and Turpin, J. A. (1997) *Antimicrob. Agents Chemother. 41*, 419−426.
28. Turpin, J. A., Terpening, S. J., Schaeffer, C. A., Yu, G., Glover, C. J., Felsted, R. L., Sausville, E. A., and Rice, W. G. (1996) *J. Virol. 70*, 6180−6189.
29. Turpin, J. A., Schaeffer, C. A., Tarpening, S. J., Graham, L., Bu, M., and Rice, W. G. (1997) *Antiviral Chem. Chemother. 8*, 60−69.
30. Tummino, P. J., Scholten, J. D., Harvey, P. J., Holler, T. P., Maloney, L., Gogliotti, R., Domagala, J., and Hupe, D. (1996) *Proc. Natl. Acad. Sci. U.S.A. 93*, 969−973.
31. Hathout, Y., Fabris, D., Han, M. S., Sowder, R. C., II, Henderson, L. E., and Fenselau, C. (1996) *Drug Metab. Dispos. 24*, 1395−1400.
32. Maynard, A. T., Huang, M., Rice, W. G., and Covell, D. G. (1998) *Proc. Natl. Acad. Sci. U.S.A. 95*, 11578−11583.
33. Chertova, E. N., Kane, B. P., McGrath, C., Johnson, D. G., Sowder, R. C., II, Arthur, L. O., and Henderson, L. E. (1998) *Biochemistry 37*, 17890−17897.
34. Huang, M., Maynard, A., Turpin, J. A., Graham, L., Janini, G. M., Covell, D. G., and Rice, W. G. (1998) *J. Med. Chem. 41*, 1371−1381.
35. Bombarda, E., Morellet, N., Cherradi, H., Spiess, B., Bouaziz, S., Grell, E., Roques, B. P., and Mély, Y. (2001) *J. Mol. Biol. 310*, 659−672.
36. Mély, Y., De Rocquigny, H., Morellet, N., Roques, B. P., and Gérard, D. (1996) *Biochemistry 35*, 5175−5182.
37. de Rocquigny, H., Ficheux, D., Gabus, C., Fournie-Zaluski, M. C., Darlix, J. L., and Roques, B. P. (1991) *Biochem. Biophys. Res. Commun. 180*, 1010−1018.
38. Ellman, G. L. (1959) *Arch. Biochem. Biophys. 82*, 70−77.
39. Griensinger, C., Otting, G., Wüthrich, K., and Ernst, R. R. (1988) *J. Am. Chem. Soc. 110*, 7870−7872.
40. Jeener, J., Meier, B. H., Bachmann, P., and Ernst, R. R. (1982) *J. Chem. Phys. 71*, 4546−4553.
41. Marion, D., and Wuthrich, K. (1983) *Biochem. Biophys. Res. Commun. 113*, 967−974.
42. Rose, G. D., Geselowitz, A. R., Lesser, G. J., Lee, R. H., and Zehfus, M. H. (1985) *Science 229*, 834−838.
43. Maret, W., and Vallee, B. L. (1993) *Methods Enzymol. 226*, 52−71.
44. Bertini, I., and Luchinat, C. (1984) *Adv. Inorg. Biochem. 6*, 71−111.
45. Chen, X., Chu, M., and Giedroc, D. P. (2000) *J. Biol. Inorg. Chem. 5*, 93−101.
46. Bertini, I., Luchinat, C., and Scozzafava, A. (1982) *Struct. Bonding 48*, 45−92.
47. Garmer, D. R., and Krauss, M. (1993) *J. Am. Chem. Soc. 115*, 10247−10257.
48. Martell, A. E., and Smith, R. M. (1974) *Critical stability constants*, Plenum Press, New York.
49. Wüthrich, K. (1986) *NMR of proteins and nucleic acids*, Wiley, New York.
50. Woolley, P. (1975) *Nature 258*, 677−682.
51. Bertini, I., Luchinat, C., Rosi, M., Sgamellotti, A., and Tarantelli, F. (1990) *Inorg. Chem. 29*, 1460−1463.
52. Pettersson, G. (1987) *CRC Crit. Rev. Biochem. 21*, 349−389.
53. Vallee, B. L., and Auld, D. S. (1990) *Biochemistry 29*, 5647−5659.
54. Merkle, D. L., Schmidt, M. H., and Berg, J. M. (1991) *J. Am. Chem. Soc. 113*, 5450−5451.
55. Klemba, M., and Regan, L. (1995) *Biochemistry 34*, 10094−10100.
56. Berg, J. M., and Merckle, D. L. (1989) *J. Am. Chem. Soc. 111*, 3759−3761.
57. Hirose, J., and Kidani, Y. (1990) in *Biocordination chemistry: coordination equilibria in biologically active systems* (Burger, K., Ed.) pp 185−235, Ellis Harwoord, New York.
58. Berg, J. M., and Godwin, H. A. (1997) *Annu. Rev. Biophys. Biomol. Struct. 26*, 357−371.
59. Maynard, A. T., and Covell, D. G. (2001) *J. Am. Chem. Soc. 123*, 1047−1058.
60. Déméné, H., Dong, C. Z., Ottmann, M., Rouyez, M. C., Jullian, N., Morellet, N., Mély, Y., Darlix, J. L., Fournié-Zaluski, M. C., Saragosti, S., and Roques, B. P. (1994) *Biochemistry 33*, 11707−11716.
61. Ramboarina, S., Morellet, N., Fournie-Zaluski, M. C., and Roques, B. P. (1999) *Biochemistry 38*, 9600−9607.
62. McLendon, G., Hull, H., Larkin, K., and Chang, W. (1999) *J. Biol. Inorg. Chem. 4*, 171−174.
63. Burgen, A. S., Roberts, G. C., and Feeney, J. (1975) *Nature 253*, 753−755.
64. Bremer, C., and Grell, E. (1996) *Inorg. Chim. Acta 241*, 13−19.
65. South, T. L., Blake, P. R., Hare, D. R., and Summers, M. F. (1991) *Biochemistry 30*, 6342−6349.

BI015956G